19th Brazilian Congress of Thermal Sciences and Engineering
November 06th-10th, 2022, Bento Gonçalves - RS - Brazil

ENC-2022-0656
NUMERICAL ANALYSIS OF FLOW OVER TWO ALIGNED CYLINDERS WITH DIFFERENT SIZES

Tainan Longo
Roberta Fatima Neumeister
Universidade Regional Integrada do Alto Uruguai e das Missões – Campus de Erechim, Erechim/RS
053540@aluno.uricer.edu.br
robertaneumeister@uricer.edu.br

Abstract. *The use of different sizes of cylinders in close space has been presented as an option to reduce the vibration amplitude of cylinders free to vibrate. This configuration can be reversed to increase the amplitude and allow energy harvesting. The present study aims to explore the flow over two aligned cylinders focusing on the fluid dynamic forces on the cylinders fixed and identifying the influence on the generating energy process. The numerical analysis is performed with a Reynolds number of 7.5 x10^4 and the space ratio equal to 2.67 for the tandem cases. The simulations were executed with the finite volumes method applying Reynolds Averaged Navier-Stokes (RANS) equations adopting the turbulence model $k\omega$ – SST. Simulations were carried out for the case of a single fixed cylinder, two cylinders with the same diameter, and two cylinders with different diameters. The results showed agreement with the literature for forces and pressure distribution. A reduction in the magnitudes of the forces was observed between the single-cylinder and the cases with pairs of cylinders, indicating that the tested configurations cannot be used as an alternative to increasing energy harvesting.*

Keywords: *cylinders, fluid-dynamic forces, numerical analysis.*

1. INTRODUCTION

The phenomenon of fluid-structure interaction called Vortex-Induced Vibration (VIV) occurs when a bluff body is immersed in a flow. The presence of the body changes the flow pattern and causes the formation of vortices. This process changes the pressure field due to the vortex formation and shedding which can cause vibrations with large amplitude if the frequency of the vortex shedding is close enough to one of the natural frequencies of the equipment (Silva, 2013).

The offshore oil extraction industry presents cylinders exposed to VIV. The connection between the platforms and the wells is through tubes known as risers. These tubes have large lengths and they present flexible characteristics, allowing oscillations and different types of vibrations that can result in fatigue damage (Freire, 2015).

The phenomenon of VIV is often linked to damage and structure problems but can be applied to harvest energy. Bernitsas et al. (2006) developed an energy hydro-collector called VIVACE, which uses vibrations induced by vortices to perform the movement of the cylinders, converting this mechanical energy, from the movement of the cylinders, into electrical energy through generators.

To reduce amplitudes in the risers or to increase amplitudes of vibration in an energy collector is necessary to understand the flow patterns and forces over one cylinder and pairs of cylinders. In the past decades, studies about the influence of many parameters on the forces over a single cylinder were presented by Zdravkovich (1997) and pairs of cylinders were presented by Zdravkovich (2002). Single-cylinder experimental analyses were performed also by Azevedo and Pinho (2011) and Gao and Liu (2018), including flow visualizations.

Alam et al. (2003) presented a study on the responses for cylinders in tandem, with an evaluation of the forces and additional parameters for a range of pitch ratios (L/D) up to 5. Silva (2013) presented a numerical study of the fluid-structure interaction of a flow around cylinders free to oscillate to better understand the phenomenon of risers. Two-dimensional and three-dimensional simulations were performed in the case of VIV around the cylinder, presenting aspects related to the models being able to capture the changes in the wake pattern, which interfered with the response of the system about the amplitude, due to the extension of the synchronization region.

Freire (2015) analyzed the VIV phenomenon with two-degrees-of-freedom cylinders in an experimental model. The experiments were carried out in a channel with recirculating water and with different conditions of inertia. He used the technique of image velocimetry of particles that allowed the identification of different vortex wake patterns. It was possible, through the experiments, to verify that the vortices do not have axial symmetry.

Campo (2015) proposed a numerical analysis of flow over two identical smooth circular cylinders with two degrees of freedom. The numerical DNS (Direct Numerical Simulation) analysis was applied to a Reynolds number between 100 and 300. The author used fixed cylinders, free in the direction transverse to the flow and free in both directions, where he noted a variation regarding the values obtained for the force coefficients, indicating that greater relations between inertial and viscous forces favor the formation and detachment of vortices. Cylinders with the freedom to vibrate in the transverse direction presented a greater relative displacement compared to the cylinder of two degrees of freedom. Lopes (2015) numerically studied the problem of vibrations due to vortex shedding. The Reynolds Number used was 200 for all cases and the cylinder movement was proposed by a system of spring-mass and damper-spring-mass. The author noted that for low values of reduced velocity, the response of the oscillating cylinder is similar to the response of the fixed cylinder, including the forces.

Paes (2018) developed the analysis on a model for vortex-induced vibrations using nonlinear oscillators to represent the dynamics in the wake of vortices in the transverse direction to the flow or the parallel direction. To examine its advantages and limitations, a calibration by comparing numerical results with experimental data was executed. The model was able to reproduce the lock-in exit region but fails to predict the maximum amplitudes for different reduced velocities.

Wang et al. (2018) presented an experimental study on the wake of two tandem cylinders of unequal diameters. The flow was classified into the reattachment and co-shedding flow regimes. It was found that the critical spacing that divides the two regimes is dictated by the upstream-cylinder vortex formation length and becomes larger for smaller d/D. Assi (2014) studied the wake-induced vibration (WIV) of the downstream cylinder of a tandem pair for different diameter ratios. The dynamic response showed that the downstream cylinder experienced WIV for all diameter ratios investigated.

Zhu et al. (2020) performed a numerical investigation for flow-induced vibration (FIV) of two rigidly coupled tandem cylinders of unequal diameters at a low Reynolds number of 150. A greater lift force exerted on the downstream cylinder had been observed, as well as the downstream cylinder had dominated the movement of the rigidly coupled cylinders in the majority of an oscillating cycle.

Farsi et al. (2022) presented an experimental analysis of the impact of cylinder transverse vibration caused by FIV to improve wind energy harvesting from these vibrations. Results show that mounting a stationary cylinder as an obstacle increases generated power efficiency to almost three times greater than a single vibrating cylinder.

The objective of the present study is to perform a numerical analysis with flow over cylinder for the configurations of single-cylinder, cylinders in tandem with equal diameter, and cylinders in tandem with different diameters. The main goal is to identify the changes in the forces between the tested cases for the same Reynolds number.

2. **METHODOLOGY**

The present numerical analysis studied three cases with fixed cylinders - details of each case are in Table 1. Case 1 is a single-cylinder, Case 2 is a pair of cylinders in the tandem configuration with the same diameter, and Case 3 is a pair of cylinders in tandem configuration with different diameters. The tandem cases present the relative pitch, L, and diameter, D, of 2.67. For Case 3 the relation between the cylinder's diameters, D_2/D_1, is 1.5. The numerical analysis is performed with water at 20 ºC and the Reynolds number for all cases is 74,108, a range classified as the subcritical regime.

To perform the numerical analysis, the initial condition was a steady-state solution. The transient analysis was performed based on the initial condition with a time step of 0.001 s. The Unsteady Reynolds Averaged Navier-Stokes (URANS) equations were solved using the k ω-SST (Shear Stress Tensor) turbulence model on the software ANSYS Fluent. The interpolation methods adopted were of second order and the residual convergence criteria were $1x10^{-5}$.

The computational domain was generated based on Silva (2013), using recommended values for the distance between the cylinder and walls. The domain's external dimensions are 500 mm x 1500 mm and a height of 500 mm. The computational domain for Case 1 and Case 3 are shown in Figures 1 a) and b).

The domain size for a single cylinder, Figure 1 a), has a blockage ratio of 15%, a distance of 6.67D from the inlet to the cylinder, and 13D after the cylinder up to the outlet. Figure 1 a) shows the top view of the domain and the distances between the cylinder and the domain boundaries for the case of a single cylinder.

Table 1. Details of the Studied Cases

Name	Description	Cylinders Diameter [m]	L/D	D_2/D_1	Reynolds Number
Case 1	Single Cylinder	0.075	-	-	74108
Case 2	Cylinders in tandem – same diameter	0.075	2.67	1	74108
Case 3	Cylinders in tandem – different diameters	0.05 – C_1 0.075 – C_2	2.67	1.5	74108

In Figure 1 b), the domain presents a 15% blockage ratio, the first cylinder is positioned at a distance of 6.67D from the inlet. The second cylinder is 2.67D from the first cylinder and 10.67D up to the end of the domain, based on the diameter value (D) of 0.075m - used as a reference.

The boundary conditions applied are indicated in Figure 1 c). For the inlet condition, a prescribed velocity with the value of 1 m/s was used. For the cylinder and the walls, the non-slip condition was assigned. For the outlet region, the condition imposed was Pressure-Outlet with atmospheric pressure.

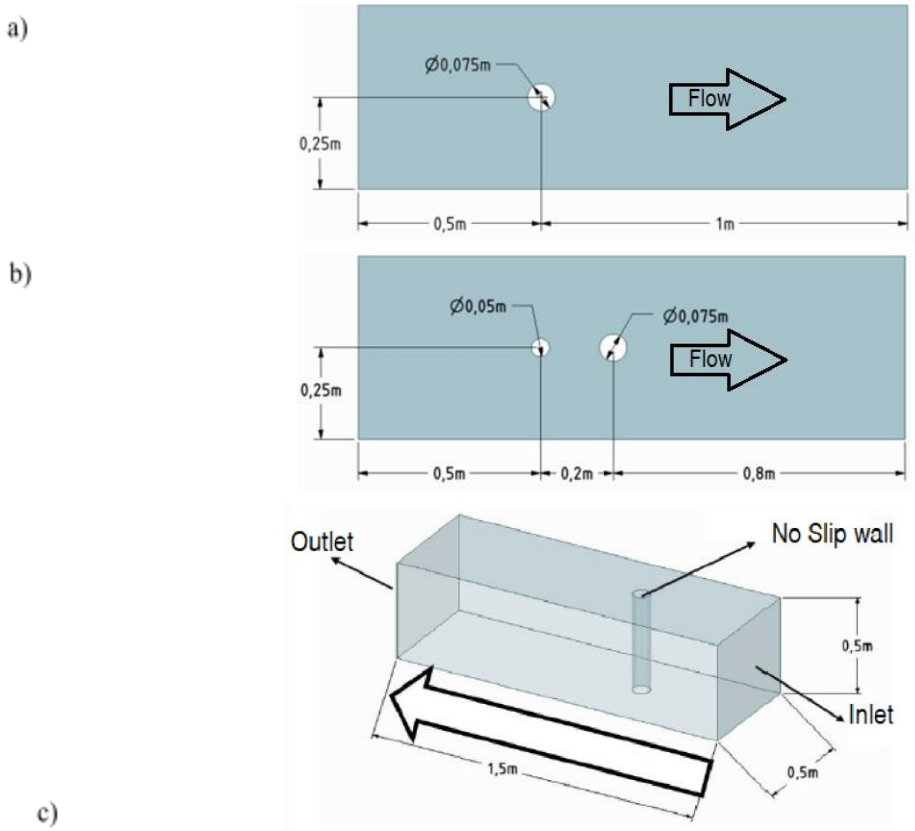

Figure 1. Numerical domain top view for Single Cylinder – Case 1 (a), Numerical domain top view for cylinders in tandem with different diameters – Case 3 (b), and Boundary conditions on the three-dimensional domain (c).

The mesh independence was executed to identify if the mesh presents an adequate number of subdivisions, being necessary to carry out several simulations for the same case. When the results do not have significant divergences, it can be assumed that the values used for the mesh generation are adequate for the study.

The drag coefficients obtained from the mesh independence cases are shown in Table 2. Similar drag coefficients were obtained with the increase in the number of volumes. It was considered that the adopted convergence criterion of $1x10^{-5}$ was suitable for the present study. For all the meshes simulated the difference between the results is lower than 1% and after the second mesh, the variation is minimal in the values found for the drag coefficient. The Mesh 03 was used in the present analysis and it is presented in Figure 2. The region around the cylinder presents a density and on the cylinder wall prismatic layers were applied to maintain y^+ under 5.

Table 2. Mesh independency analysis

Mesh	Number of volumes	C_d	Difference %
01	3 mi	0.9987	0.82%
02	4 mi	0.9905	0.18%
03	6 mi	0.9887	0.09%
04	8 mi	0.9878	-

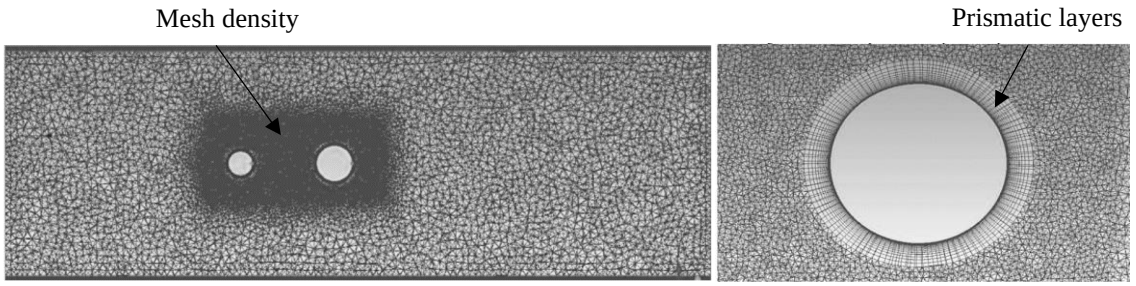

Figure 2. Mesh used in the simulation with cylinders in tandem with different diameters a) Mesh in all the domains and b) Detail of the mesh around the cylinder with prismatic layers.

3. **RESULTS**

The results are presented for each case separated. In section 3.1 the results are shown from one single cylinder, in section 3.2 the results for cylinders in tandem with equal diameter can be observed and in section 3.3 the results for cylinders in tandem with different diameters are presented. The comparison with literature results and discussion of present responses are executed along with the results.

3.1**Case 1 - Single Cylinder**

The flow around a single fixed cylinder was carried out in a transient regime, the drag coefficient, lift coefficient, and pressure distribution were monitored over time. The analysis was performed for a flow in the water with a Reynolds number of 74,108. The wake formation and some flow characteristics were analyzed and are presented with streamlines in Figure 3 a). The results present similarities compared with Gao and Liu (2018) where visualizations for Re = 25,700 were executed. The main structures on the flow and wake are similar, the separation point is observed at a higher angle from the separation point for the present simulation, indicating a reduction in the drag coefficient due to the reduction of the wake and related to the increase in the Reynolds Number.

The results for drag coefficient, lift coefficient, and Strouhal number are presented in Table 3. The values obtained for the present analysis, with a single cylinder, are $C_d = 0.98$, $C_l = 0.6$, and $St = 0.19$. The comparison with the results presented by Azevedo and Pinho (2011) and Zdravkovich (1997) are shown in Table 3. According to the values presented, it is possible to notice a similarity in the drag coefficient found by Azevedo and Pinho (2011). Comparing the result of the drag coefficient with Zravkovich (1997), for the Reynolds number of $7.4 x10^4$, the values obtained for the drag coefficient were 11% lower. The lift coefficient also presented lower values in the present analysis compared to Azevedo and Pinho (2011). The Strouhal number is lower than the results obtained by Azevedo and Pinho (2011). The difference observed in

the present results can be linked to the Reynolds number range which is higher than the compared data. Another factor is the blockage ratio which changes from 15% in the present analysis to values under 10% in the other cases.

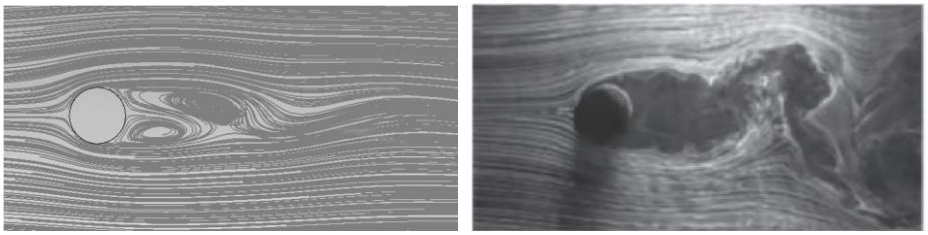

a) b)

Figure 3. Top view with the flow around single-cylinder a) Case 1 and b) Single cylinder visualization adapted Gao and Liu (2018)

Table 3. Strouhal number, drag and lift coefficients.

	Re	C_d	C_l	St
Case 1	74108	0.98	0.6	0.19
Azevedo and Pinho (2011)	27400	1.053	0.965	0.22
Zdravkovich (1997)	74000	1.1	-	-

The pressure distribution around the single cylinder is presented in Figure 4, it is possible to observe the behavior of the pressure on the cylinder. The pressure field varies over time and the force result is given by the integration of the pressure field that acts on the body. The force is divided between the force perpendicular to the flow (FL) and the force parallel to the flow direction (FD). The pressure coefficient shows agreement with the distributions presented by Zdravkovich (1997), wherein the flow incident angle the C_p is equal to one and reduces up to C_p = -2, after the separation point the pressure increases and stabilizes around C_p = -1.3. Case 1 was simulated to identify the parameters of force, vortices detachment, and flow pattern without perturbations from other bodies.

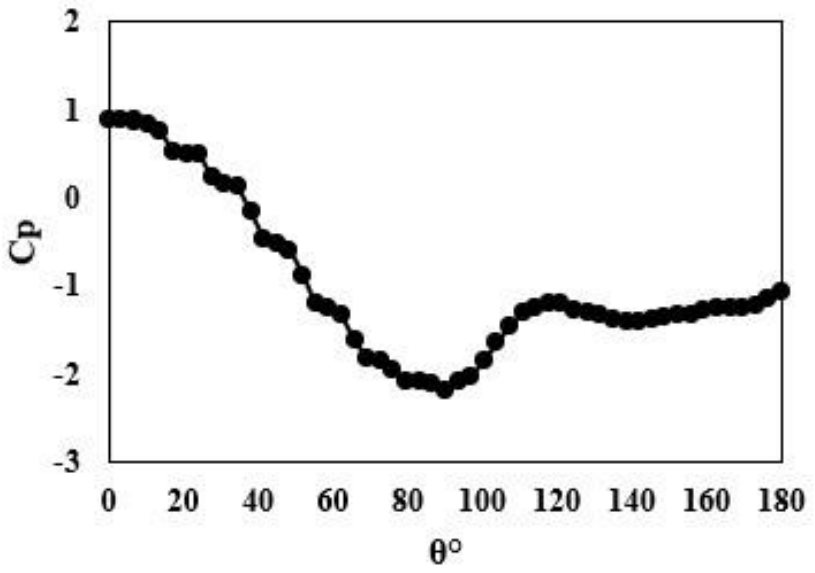

Figure 4. Pressure coefficient on the single-cylinder (Case 1).

3.2**Case 2 - Tandem cylinders with equal diameters**

The analysis with crossflow over two cylinders in tandem with the same diameter was performed in a transient regime for Re = 74,108. The drag and lift coefficients in both cylinders were monitored, and the pressure distribution on the cylinders was evaluated. The flow pattern and structures were monitored and are presented in Figure 5. The results in Figure 5 a) are related to the present analysis and the reattachment of the first cylinder shear layers is observed in the second cylinder, this is a characteristic that can or not happen on the space ratio over 2.5 (Alam et al.,2003). In Figure 5 b) the visualization from Wang et al. (2018), for tandem configuration and pitch ratio 2.5 is observed, in this case, the reattachment of the shear layer is also observed. In Figure 5 is observed that the first cylinder wake is larger and englobe the second cylinder, while the second cylinder presents a smaller wake.

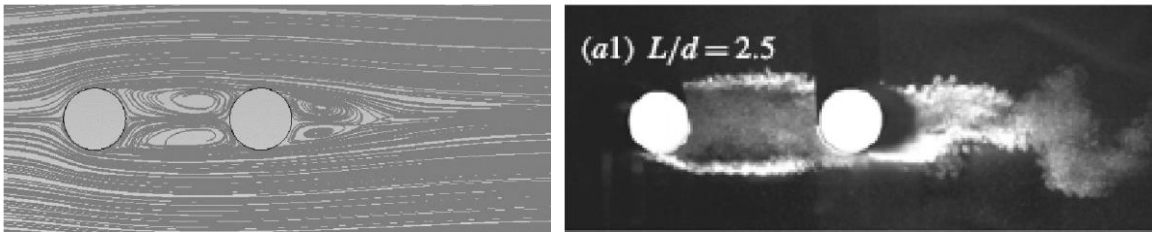

Figure 5. Top view with the flow around cylinders in tandem same diameters a) Case 2 and b) tandem L/D=2.5, adapted from Wang et al. (2018)

The results of C_d, C_l, and St from the present analysis, Silva (2008) and Alam et al. (2003) are in Table 4. The values are presented for the first cylinder, C_1, and the second cylinder, C_2. The drag coefficient in C_2 is lower than on C_1 and in opposite direction, this can be associated with the fact that cylinder C_2 is in a region wake of C_1 and will strongly interfere with the pressure distribution over C_2. In this case, the second cylinder presents a force moving it towards the first cylinder.

Comparing the value of C_d obtained for C_1 with the results from Silva (2008) and Alam et al. (2003) it is observed that the value obtained is 21% and 26% lower for cylinder C_1, respectively. The space ratio is not the same for all the cases and this influences the response, as can be observed in the second cylinder where the results from Silva (2008) present positive drag coefficients while the present results and the results from Alam et al. (2003) show negative drag coefficients.

Alam et al. (2003) presented a map relating C_d and L/D, where, for an L/D equal to 3, there is an increase in the values of C_d, representing the shear layer separating from the upstream cylinder and reconnecting to the surface of the downstream cylinder, occurring a bifurcation in two shear layers at the point of replacement. For an L/D of 2.67, the values for cylinder C_1 have a variation of around 20% and for C_2 these values of C_d are similar and are negative as shown in Table 4.

The results for C_1 and C_2 presented lower values than Alam et al. (2003) with 35% and 39%, respectively. The value of the number of Strouhal for tandem configuration and space ratio 2.67 is in the range of 0.11 to 0.22 (Zdravkovich, 2002). The values for cylinders C_1 and C_2 were between the range of values and are shown in Table 4.

Table 4. Strouhal number, drag and lift coefficients.

Description			C_1			C_2		
	Re	L/D	C_d	C_l	S_t	C_d	C_l	S_t
Case 2	74,108	2.67	0.64	0.18	0.086	-0.22	0.23	0.163
Silva (2008)	78,960	2	0.812	-	0.2041	0.32	-	0.204
Alam et al. (2003)	65,108	2.5	0.86	0.28	0.14	-0.2	0.38	0.14

Both C_d and C_l for the first cylinder had variations compared to Case 1, Table 3, indicating that the downstream cylinder, C_2, interfered in the development of the wake and flow for both cylinders. The magnitudes of the force coefficient were reduced for Case 2 compared with Case 1. Considering the energy generation by vibrations in these cylinders, the

configurations used for Case 2 do not increase these forces over the cylinders. This relation can be made due to Lopes (2015) studies that showed that the forces are equivalent in fixed and free to vibrate cylinders in low reduced velocities.

The pressure distribution over the cylinders is presented in Figure 6 for Case 2. The pressure coefficients for cylinder 1 present a higher range (1.1 to -1.3) than cylinder 2 (0.8 to -0.95). The response of cylinder 1 compared to Case 1, shows the influence of the downward cylinder in the pressure distribution. The separation point is at a higher angle for the second cylinder than the first one. The results are following the results presented by Alam et al. (2003) for pressure distribution.

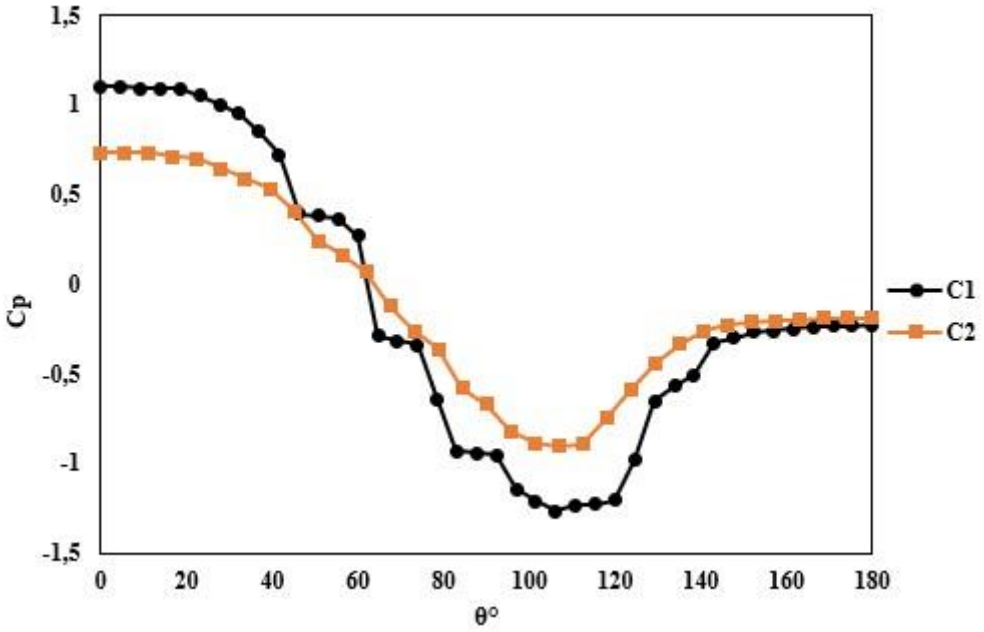

Figure 6. Pressure coefficient on the cylinders in tandem with the same diameter (Case 2).

3.3**Case 3 - Tandem cylinders with different diameters**

The analysis with crossflow over two cylinders in tandem with different diameters was performed in a transient regime for Re = 74,108, with the second cylinder presenting 1.5 times the diameter of the first cylinder. The drag and lift coefficients in both cylinders were monitored and the pressure distribution on the cylinders was evaluated. The flow pattern and structures were monitored and are presented in Figure 7. In Figure 7 a) the results from the present analysis show the reattachment of the first cylinder shear layers on the second cylinder. It also presents the influence of the main flow over the second cylinder with the non-perturbed flow. In Figure 7 b), a visualization for L/D = 3 from Wang et al. (2018) is presented and the similarity in the flow with the present case can be observed. Compared with the results from Cases 1 and 2, Figure 3 and Figure 5, a change in the main structures can be observed, resulting from the change in the diameter of cylinder C_1, which causes the flow to change the main structures.

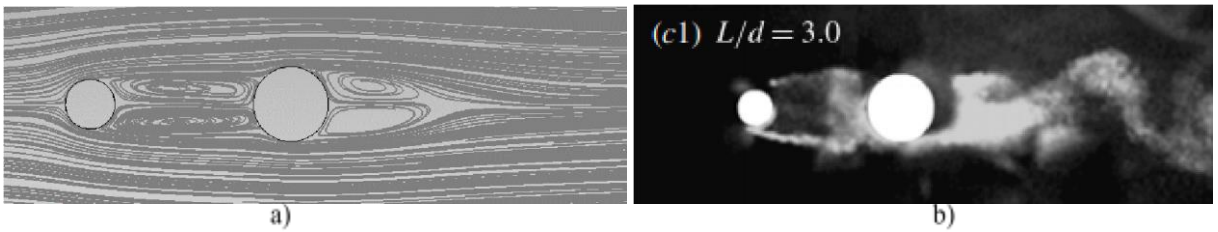

Figure 7. Top view with the flow around cylinders in tandem same diameters a) Case 2 and b) tandem L/D=3 adapted from Wang et al. (2018)

Table 5 presents the values of the drag and lift coefficients obtained for this study and the results presented by Assi (2014) to compare. The drag coefficient obtained for C_1 is in the same range that the result in Case 2 but is lower than the

single cylinder case (Case1), due to the interference of the downstream cylinder. The results in C_2 showed the value of C_d higher in Case 3 than in Case 2. The differences observed between Case 2 and Case 3 occurred due to the C_1 smaller diameter for Case 3 (0.05 mm), and part of the flow collides with the frontal region of cylinder, C_2, generating a larger contact area with the main flow.

The values presented by Assi (2014) showed higher magnitudes than the present case but the same tendency with higher coefficients in the first cylinder and lower in the second cylinder. The lift coefficients in Case 3, where the cylinders present different diameters, showed similar values observed in Case 2 but with lower magnitudes than the ones observed in the single cylinder case. The values presented by Assi (2014) showed the first cylinder with a higher lift force than the second cylinder.

The pressure distribution over the cylinders is presented in Figure 8 for Case 3. The pressure coefficients for cylinder 1 present a higher range than cylinder 2, but the lower levels of pressure and the points of separation are equivalent.

Table 5. Strouhal number, drag and lift coefficients.

	Re		C_d	C_l	St
Case 3	74108	C_1=0.05	0.61	0.298	0.12
		C_2=0.075	0.405	0.245	0.18
Assi (2014)	49000	C_1=0.025	0.979	0.52	0.21
		C_2=0.05	0.81	0.35	0.2

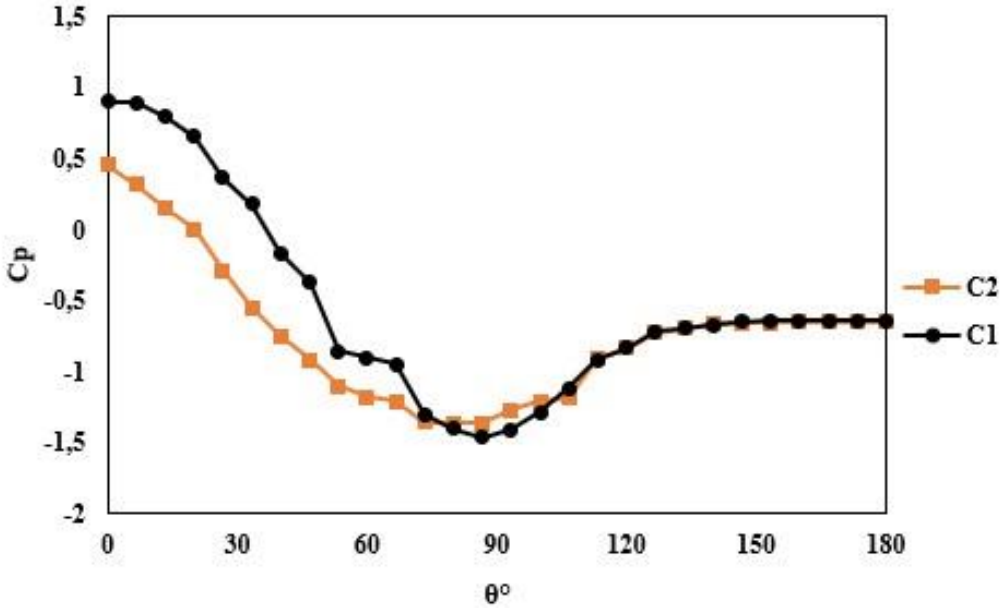

Figure 8. Pressure coefficient on the cylinders in tandem with the different diameters (Case 3).

4. CONCLUSIONS

The present study showed results of a crossflow over a single cylinder, two cylinders in tandem with equal diameters, and two cylinders in tandem with different diameters. For all the cases the study is in the transient regime for Re = 7.4 x 10^4. The cases were analyzed with drag and lift coefficients and the pressure distribution on the cylinders.

The results for all the cases were compared to the literature information and showed equivalences in the tendency of the forces coefficients and the flow patterns, although the results did not increase the force coefficient with the addition of the cylinder. The space ratio tested was 2.67 and two main patterns can be observed in this configuration (Wang et al. ,2018), the reattachment and co-shedding, in the present results the reattachment pattern was observed.

The drag forces showed higher values for Case 1, single-cylinder, than for Case 2 and Case 3. The case with both cylinders of the same size (Case 2) presented a negative drag force in the second cylinder, this response was associated with the interaction of the first cylinder wake.

The lift forces presented lower values for the cases with pairs of cylinders, even with the change in the pressure distribution generated by the addition of a cylinder in the interaction region. The pressure coefficient showed that the presence of the upward cylinder changed the separation angle and showed a smaller range for the pressure coefficients on the pairs of cylinders results.

The tested cases showed a decrease in the lift forces magnitudes which would be a reduction in the excitation of the cylinder free to vibrate to the energy harvesting. The range of Strouhal numbers is the same for the cases in tandem with equal or different diameters indicating that these configurations are not a good option to improve vibration. The increase in the pitch ratio is an alternative to future works, once the excitation mechanism presents a well-defined frequency linked to the first cylinder wake.

REFERENCES

Alam, M. M., Moriya, M., Takai, K., & Sakamoto, H., 2003. "Fluctuating fluid forces acting on two circular cylinders in a tandem arrangement at a subcritical Reynolds number". *Journal of Wind Engineering and Industrial Aerodynamics*, 91(1-2), 139-154.

Assi, G. R. 2014. Wake-induced vibration of tandem cylinders of different diameters. *Journal of Fluids and Structures*, 50, 329-339.

Azevedo, M. A.; Pinho, F., 2011. *Simulação Numérica Do Escoamento Em Torno de Um Cilindro A Número De Reynolds Moderado: Comparação Entre Alguns Modelos De Turbulência.* CIBEM. Faculdade de Engenharia Mecânica de Porto. Portugal, Universidade Politécnica do Noroeste China, 2018.

Bernitsas, M. M., Raghavan, K., Ben-Simon, Y., & Garcia, E. M. H., 2006. "VIVACE (vortex-induced vibration aquatic clean energy): a new concept in generation of clean and renewable energy from fluid flow". *International Conference on Offshore Mechanics and Arctic Engineering* Vol. 47470, pp. 619-637.

Campo, G. F., 2015. *Análise numérica da vibração induzida por vórtices de dois cilindros alinhados com o escoamento*. Dissertation, Universidade Federal do Rio Grande do Sul.

Farsi, M., Shariatzadeh, M. J., Bijarchi, M. A., Pournasiri Masouleh, E., and Shafii, M. B. (2022). Low-speed wind energy harvesting from a vibrating cylinder and an obstacle cylinder by flow-induced vibration effect. International Journal of Environmental Science and Technology, 19(3), 1261-1272.

Freire, C. M, 2015. *Estudo experimental do fenômeno de vibração induzida por vórtices em cilindro rígido livre para oscilar com dois graus de liberdade* (Doctoral dissertation, Universidade de São Paulo).

Gao, N.; Liu, X. H. 2018. *An improved smoke-wire flow visualization technique using capacitor as power source*. Theoretical and Applied Mechanics Letters, 8(6), 378-383.

Lopes, R. M. V, 2015. *Estudo numérico do fenómeno de vibração induzida por vórtices num cilindro com 1 grau de liberdade em OpenFoam* (Doctoral dissertation).

Paes, C. B., 2018. *Análise De Vibrações Induzidas Por Vórtices Usando Osciladores Não-Lineares* (Doctoral dissertation, Universidade Federal do Rio de Janeiro).

Silva, A. R., 2008. *Modelagem Matemática de Interação Fluido-Estrutura Utilizando o Método da Fronteira Imersa*. Tese (Doutorado em Engenharia Mecânica). Universidade Federal de Uberlândia. Uberlândia – MG.

Silva, D. R. B., 2013. *O conceito de inércia adicional do escoamento em torno de cilindro circular em oscilação forçada* (Doctoral dissertation, Universidade de São Paulo).

Wang, L., Alam, M. M., and Zhou, Y. 2018. Two tandem cylinders of different diameters in cross-flow: Effect of an upstream cylinder on wake dynamics. *Journal of Fluid Mechanics*, 836, 5-42.

Zdravkovich, M. M., 1997. *Flow around circular cylinders. Fundamentals*, Volume 1, Oxford University Press.

Zdravkovich, M. M. 2002. *Flow around circular cylinders: Applications*, Volume 2. Oxford University Press.

Zhu, H., Tan, X., Gao, Y., Zhou, T., and Liu, W. 2020. Two-degree-of-freedom flow-induced vibration of two rigidly coupled tandem cylinders of unequal diameters. Ocean Engineering, 216, 108142.

5. RESPONSIBILITY NOTICE

The authors are the only ones responsible for the printed material included in this paper.